

A novel type compact five-coordinate measuring machine with laser and CCD compound probe

Z G Fei^{12*}, J J Guo¹, X J Ma³, D Z Gao³

1, State Key Laboratory for Manufacturing Systems Engineering, Xi'an Jiaotong University, Xi'an, China

2, Mechanical & Electrical Engineering Department Zhengzhou University of Light Industry, Zhengzhou, China

3, Research Center of Laser Fusion, CAEP, Mianyang, China

Abstract: In this paper, a novel type compact five-coordinate measuring machine with laser and CCD compound probe, which consists of three translational axes and two rotational axes, was designed and built. According to the structure and coordinate relationship of this machine, its measurement mathematical model is established. The genetic algorithm is applied to solve the unknown parameters of the model. Hence, by means of this model, the 3D surface data of the tested object can be transformed into the same reference coordinate system. Quasi-Newton method is introduced and in charge of processing these surface data. Based on the variety of tested object, such as plane, sphere, cylinder etc. the corresponding optimization objective function and initial condition are set properly to achieve the solution of characteristic parameters. Especially, in this work, an evaluation function method based on the "roundness" information of the image of through-hole is proposed to detect the diameter and spatial location of hole, which particularly fits for inspecting those thin and small through-holes drilled at the soft and easy-deformed objects. Consequently, the measurement puzzle of spatial angle between two thin and through-holes is easily solved. The experiments show that the measurement repeatability of this machine is within $1.6\ \mu\text{m}$, which can meet the measurement requirement very well. Meanwhile, the experiments illustrate the validity and feasibility for through-holes measurement.

Keywords: Five-coordinate measuring machine, Measurement model, Parameter calibration, Quasi-Newton method, Through-hole measurement

1 INTRODUCTION

At present, CMM is proceeding at the direction of high-speed, miniaturization, high-precision and non-orthogonalization[1]. Owing to its inherent limitation, the traditional contact CMM fails to measure those tiny holes and slots, as well as those soft and easy-deformed objects. Hence, the exploitation of multi-coordinate and non-contact CMMs shows its necessity increasingly, which will enhance the flexibility of CMMs largely [2].

Especially for such specific kind of objects with tiny dimensions and complex shapes, both their 3D geometric dimensions and relative spatial position of each part are required to be tested. The existing CMMs are mainly three-coordinate measuring machines, which are difficult even fail to meet such specific measurement task.

To cope with this kind of task, a compact five-coordinate measuring machine is designed and built, in which several key technologies are

* Corresponding author: School of Mechanical Engineering,

Institution of Precision Engineering, 28 Xianning West Road,
Xi'an, People's Republic of China.

email: fzg2006@stu.xjtu.edu.cn

adopted, such as the latest digital measurement technique, high-precision mechanical structure, laser probe and CCD aiming technique, mature distributed motion control technique and data optimization processing technique.

In the following sections, several problems, such as the mechanical structure, the control system, the measurement model establishment, the geometric parameters calibration, and data processing algorithm, are discussed in detail. It is worth mentioning that the dimension and spatial location measurements of thin and soft holes are still a puzzle so far. By combining with the structure form of this machine, this paper introduces a new method based on the “roundness” evaluation of tested hole, which succeeds in solving this problem. Finally, the related experiments illustrate the characteristics of this machine as well as the feasibility and validity of mentioned algorithms.

2 THE MECHANICAL STRUCTURE AND CONTROL SYSTEM

2.1 The mechanical structure

By comparison, the structure form of base and cantilever beam is selected as the mechanical structure of this machine presented in Fig.1. The laser displacement sensor and CCD camera compose the compound probe, which is located at the front of cantilever beam and can rotate around A and B axes while moving along Z axis. The tested object lies on the worktable which can travel along X axis and Y axis in horizontal direction. The step motors with subdivision function are applied to drive each axis. Among them, the motor for A axis has contracting brake device which will lock the motor mainshaft and prevent collision of the probe and worktable in case of accidental power off. The high-precision ball screws are used to drive X and Y axes. Considering the layout rationality of motor, the transmission of Z axis adopts the hybrid form of synchronous belt and ball screws. The motor for A axis drives the probing system with planetary gear reducer

directly. The motor for B axis drives the compound probe through planetary gear reducer and synchronous belt. Meanwhile, in order to balance the gravity effect of beam components, a sixteen kilogram counterweight is hanging behind the column. The materials of the base and column are both natural marble because of its outstanding stability.

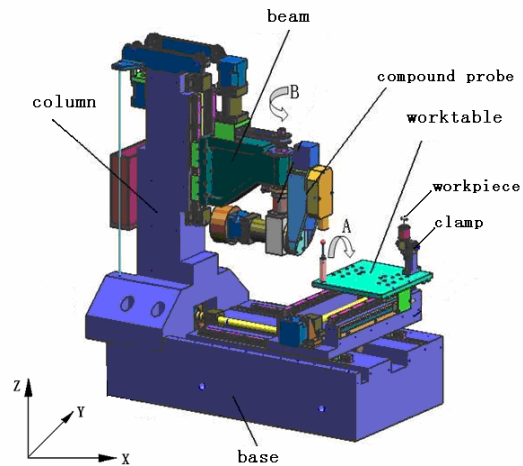


Fig.1 The overall mechanical structure.

The prominent advantage of such structure lies in the fact that the object can be detected from different directions as extensively as possible. Compared to the existing three-coordinate measuring machine, no doubt, this five-coordinate measuring machine increases measurement flexibility. It is easier to acquire more detail information of objects. Also, because of its non-contact measurement, there is no worry to damage the tested objects. The strokes of A and B axes are $\pm 120^\circ$ and $\pm 90^\circ$ respectively. The ones of XYZ axes are $200\text{mm} \times 160\text{mm} \times 60\text{mm}$. As an example of measuring sphere surface, this machine is able to scan two thirds of the sphere surface by means of five axes linkage motion. Shown in Fig.2, the rest surface can be inspected easily except for the red shade area. To some extent, increase the height of the clamp, the measurable area will be larger.

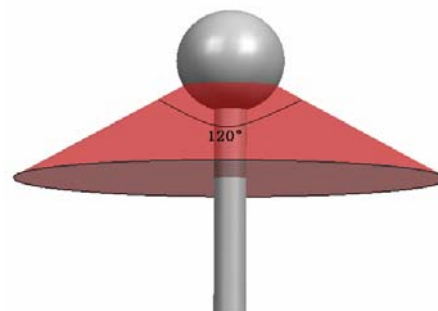


Fig.2 The measurable area and unmeasurable area

The compound probe includes laser displacement sensor and CCD camera shown in Fig.3. As we all know, laser probe has high sensitivity and measurement precision in its axial direction, in the meantime, CCD can reach pretty high measurement precision for 2D image. Combined with both their merits, that is why the compound probe is adopted.

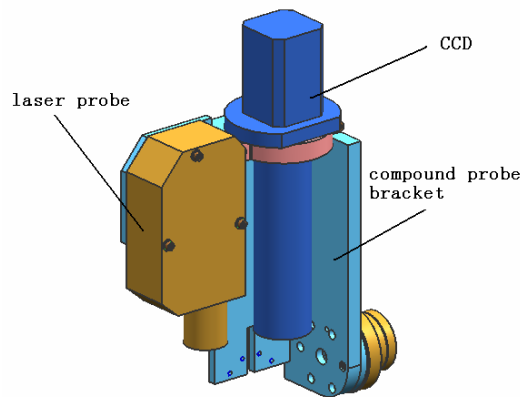


Fig.3 The compound probe

2.2 The control system

Fig.4 illustrates the composition of control system of this machine clearly. The entire control system consists mainly of the host computer, DSP motion control card, servo system and manipulating box. The distributed closed-loop control model is applied in which motors drive moving parts and gratings detect the position of moving parts. The host computer communicates with motion control card by Ethernet cable. During the measurement course, the motion control card is in charge of five axes' motion. Both single-axis motion and multi-axis synchronous motion can be realized. Meanwhile, the host computer reads the measured value of laser probe through Ethernet cable and receives the image information from CCD through 1394 interface.

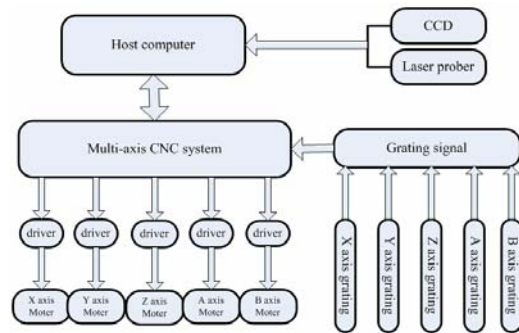


Fig.4 The frame diagram of control system

3 THE MEASUREMENT MODEL AND SYSTEM GEOMETRIC PARAMETERS CALIBRATION

First of all, at the beginning of measurement, the establishment of system measurement model is necessary. At the same time, owing to the installation and assembly error, the accurate calibration of system geometric parameters is also necessary.

3.1 The establishment of measurement model

Based on the structure form of this machine, four coordinate systems are introduced in Fig.5.

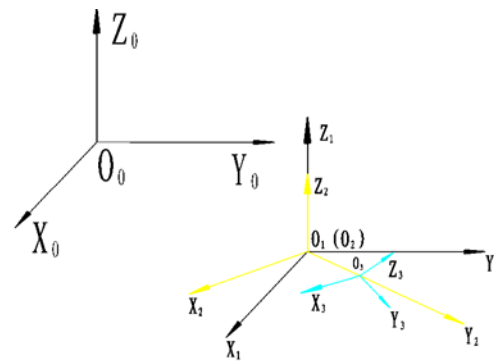


Fig.5 The relationship of four coordinate systems

1) The machine coordinate system

$O_0X_0Y_0Z_0$.

2) The machine moving coordinate system $O_1X_1Y_1Z_1$. Its origin O_1 is the intersection point of the centerline of B axis and the horizontal plane containing the centerline of A axis. It doesn't change with the movement of each axis. The directions of its three axes are same with the ones of machine coordinate system.

3) The coordinate system $O_2X_2Y_2Z_2$ based on B axis. Its origin is same with O_1 . Its

Z_2 axis is parallel to the Z axis of machine coordinate system. Its axis X_2 is parallel to the centerline of A axis. The direction of axis Y_2 is derived by right-hand rule.

4) The coordinate system $O_3X_3Y_3Z_3$ based on A axis. The direction of axis X_3 is same with axis X_2 . The direction of axis Z_3 is the one of axis Z which has rotated around A axis at a given angle. Its origin O_3 is the intersection point of X_3 and Z_3 . The direction of axis Y_3 is derived by right-hand rule.

Analyzing the relationship among these four coordinate systems, There is a translation relationship between coordinate $O_1X_1Y_1Z_1$ and $O_0X_0Y_0Z_0$. The translation matrix is T_{10} .

$$T_{10} = Q_{10} \quad (1)$$

where $Q_{10} = [x_{10}, y_{10}, z_{10}]^T$, which are the grating readings of XYZ axes.

There is an only rotation matrix around Z axis between $O_2X_2Y_2Z_2$ and $O_1X_1Y_1Z_1$.

$$T_{21} = R_{21} \quad (2)$$

Here,

$$R_{21} = \begin{bmatrix} \cos(\theta_B + \Delta\theta_B) & -\sin(\theta_B + \Delta\theta_B) & 0 \\ \sin(\theta_B + \Delta\theta_B) & \cos(\theta_B + \Delta\theta_B) & 0 \\ 0 & 0 & 1 \end{bmatrix},$$

θ_B is the rotation angle of B axis relative to measurement zero position. $\Delta\theta_B$ is a deviated angle of the centerline of A axis motor relative to measurement zero position, which is a very small given value usually.

There is a translation and rotation relationship between $O_3X_3Y_3Z_3$ and $O_2X_2Y_2Z_2$.

$$T_{32} = R_{32} + Q_{32} \quad (3)$$

$$\text{Here, } R_{32} = \begin{bmatrix} 1 & 0 & 0 \\ 0 & \cos \theta_A & -\sin \theta_A \\ 0 & \sin \theta_A & \cos \theta_A \end{bmatrix},$$

$Q_{32} = [0, \Delta y_{32}, 0]^T$. Δy_{32} is a translation value between the origins O_3 and O_2 .

In the coordinate system $O_3X_3Y_3Z_3$, the optical axis equation of the laser probe is determinate. By assuming that $q(x, y, z)$ is the measured point, (x_{43}, y_{43}, z_{43}) are the coordinates of zero position of laser probe, the orientation vector of the optical axis is

(l, m, n) . If the reading of laser probe is t , the line equation of optical axis will be presented below.

$$\frac{x - x_{43}}{l} = \frac{y - y_{43}}{m} = \frac{z - z_{43}}{n} = t \quad (4)$$

Thus, the coordinates of q are written as follow in the $O_3X_3Y_3Z_3$.

$$\begin{bmatrix} x_q \\ y_q \\ z_q \end{bmatrix} = \begin{bmatrix} tl + x_{43} \\ tm + y_{43} \\ tn + z_{43} \end{bmatrix} = t \cdot R_{43} + Q_{43} \quad (5)$$

here, $R_{43} = [l \ m \ n]^T$, $Q_{43} = [x_{43} \ y_{43} \ z_{43}]^T$.

By means of coordinate transformation relationship, the reading of laser probe can be transformed into the machine coordinate system $O_0X_0Y_0Z_0$. Suppose the current reading of laser probe is t , its corresponding coordinates are $(x_{q0}, y_{q0}, z_{q0})^T$ in the machine coordinate system. Substitute equation (1)-(5) into equation (6).

$$\begin{bmatrix} x_{q0} \\ y_{q0} \\ z_{q0} \end{bmatrix} = T_{10} \cdot T_{21} \cdot T_{32} \cdot \begin{bmatrix} x_q \\ y_q \\ z_q \end{bmatrix} \quad (6)$$

Equation (7) can be obtained after the simplification of equation (6).

$$\begin{bmatrix} x_{q0} \\ y_{q0} \\ z_{q0} \end{bmatrix} = R_{21} \cdot (R_{32} + Q_{32}) \cdot (t \cdot R_{43} + Q_{43}) + Q_{10} \quad (7)$$

Equation (7) is right the measurement model of this machine.

3.2 The calibration of system geometric parameters

In equation (7), the solution of unknown parameters can get help from measuring a given spatial point, such as the center of a standard ball. Obviously, when the laser probe reaches a specific location, the angle θ_A and θ_B is known and unchanged. Then the value of $R_{21} \cdot (R_{32} + Q_{32}) \cdot (t \cdot R_{43} + Q_{43})$ is denoted as $(\Delta x, \Delta y, \Delta z)^T$.

$$\begin{bmatrix} x_{q0} \\ y_{q0} \\ z_{q0} \end{bmatrix} = \begin{bmatrix} \Delta x \\ \Delta y \\ \Delta z \end{bmatrix} + \begin{bmatrix} x_{10} \\ y_{10} \\ z_{10} \end{bmatrix} \quad (8)$$

From equation (8), when the laser probe is in a given posture, scan a standard ball with the

laser probe and obtain its center S_1 .

$$S_0 = S_1 + (\Delta x, \Delta y, \Delta z)^T \quad (9)$$

Here, $S_0(x_0, y_0, z_0)$ denote the ball center coordinates in the machine coordinate system. So, if the laser probe scans the standard ball once in one posture, three equations will be established. Consequently, the measurement data in four postures is enough to solve eight unknown parameters in the measurement model and three ball center coordinates (x_0, y_0, z_0) .

In addition, because R_{43} is an unit vector, a constraint equation is added. Construct the objective function as follows.

$$\begin{cases} F(X) = \sum_{i=1}^n \|S_0^{(i)} - S_0\|^2 = \min \\ h = l^2 + m^2 + n^2 - 1 = 0 \end{cases} \quad (10)$$

Transform the constraint optimization function into the nonrestraint optimization function by means of the penalty function.

$$G(X) = \sum_{i=1}^n \|S_0^{(i)} - S_0\|^2 + M \cdot h^2 \quad (11)$$

where, n is the measurement times. M says the penalty factor.

3.3 The genetic algorithm

In order to identify and calibrate the unknown system parameters, an improved genetic algorithm is adopted in this work.

(1) Coding. Here real number coding is applied to prevent the occurrence of "Hamming cliff".

(2) Generate the initial population with N samples at random.

(3) Design the fitness evaluation function as follows.

$$Fit(X) = \frac{1}{1 + G(X)} \quad (12)$$

From the definition of objective optimization function, it is clear that $Fit(X) \geq 0$.

(4) The selection operator adopts the elitist strategy. Besides, two-point crossover operator and Gaussian mutation operator are used for the population.

(5) Iteration termination judgment. If the value of $Fit(X)$ is less than 10^{-6} or the

maximum evolution generations reach 1000, terminate the iteration.

3.4 The location relationship calibration between laser probe and CCD

By means of above system measurement model, the readings of laser probe can be transformed into the machine coordinate system successfully. How to transform the data captured by CCD in the same way? The location relationship calibration between laser probe and CCD is necessary.

Firstly, under the zero position posture of AB axes, scan the standard ball with laser probe. The ball center coordinates (x_{01}, y_{01}, z_{01}) can be achieved by least square method.

Secondly, extract the edge information of this standard ball outer circle with CCD. Then, this circle center (x_{02}, y_{02}) can be obtained by fitting method. Therefore, the location relationship between two optical axes may be written as below.

$$\begin{aligned} \Delta x_0 &= x_{02} - x_{01} \\ \Delta y_0 &= y_{02} - y_{01} \end{aligned} \quad (13)$$

4 THE QUASI-NEWTON METHOD

After the surface point acquisition of tested object is completed, it is need to select a method to process these data and obtain the characteristic parameters of tested object. Quasi-Newton method is employed here. As an unconstrained optimization algorithm, Quasi-Newton method is by far the most effective optimization algorithm with fast convergence speed, high stability, easy programming [3,4].

By assuming that the solution is x_{k+1} after k th iteration, the objective function $f(x)$ is expanded into Taylor series at x_{k+1} , take its second-order approximation as.

$$f(x) \approx f(x_{k+1}) + \nabla f(x_{k+1})(x - x_{k+1}) + \frac{1}{2}(x - x_{k+1})^T \nabla^2 f(x_{k+1})(x - x_{k+1}) \quad (14)$$

Hence,

$$\nabla f(x) \approx \nabla f(x_{k+1}) + \nabla^2 f(x_{k+1})(x - x_{k+1}) \quad (15)$$

Let $x = x_k$, then

$$\nabla f(x_{k+1}) - \nabla f(x_k) \approx \nabla^2 f(x_{k+1})(x_k - x_{k+1}) \quad (16)$$

Introduce the symbol s_k and y_k .

$$s_k = x_{k+1} - x_k, y_k = \nabla f(x_{k+1}) - \nabla f(x_k)$$

At the same time, assume the matrix $\nabla^2 f(x_{k+1})$ is invertible, equation (16) is presented as:

$$s_k \approx [\nabla^2 f(x_{k+1})]^{-1} y_k \quad (17)$$

Therefore, as long as the first order derivative of objective function is solved, the inverse of the Hessian matrix can be estimated based on equation (17). Here H_{k+1} must satisfy

$$s_k \approx H_{k+1} y_k \quad (18)$$

With regard to the constitution of matrix H_{k+1} , the most widely used the Broyden-Fletcher-Goldfarb-Shanno(BFGS) formula is adopted here[5].

$$H_{k+1} = H_k + [1 + \frac{y_k^T H_k y_k}{s_k^T y_k}] \frac{s_k s_k^T}{s_k^T y_k} - \frac{s_k y_k^T H_k}{s_k^T y_k} \quad (19)$$

Algorithm steps:

(1) According to the measured object, construct the objective function $f(x)$.

(2) Give initial point x_0 , while set convergence condition $\varepsilon, k = 0$.

(3) Suppose $H_0 = I$, compute the gradient value $g_k = \nabla f(x_k)$ of $f(x)$ at x_k .

(4) Determine the searching direction $d_k = H_k g_k$.

(5) Starting from x_k , make a one-dimensional search along d_k , and meets

$$f(x_k + \lambda_k d_k) = \min_{\lambda \geq 0} f(x_k + \lambda d_k)$$

Let $x_{k+1} = x_k + \lambda_k d_k$.

(6) If $\|f(x_{k+1})\| < \varepsilon$, stop the iteration, achieve the optimal solution $x = x_{k+1}$, else turn to step (7).

(7) If $k = N - 1$, let $x_0 = x_{k+1}$, return step (3), else turn to step (8).

(8) Let $g_{k+1} = f'(x_{k+1}), s_k = x_{k+1} - x_k, y_k = g_{k+1} - g_k$, calculate H_{k+1} with equation (19). Assume $k = k + 1$, return step (4).

Aiming at different tested objects, we should set corresponding objective function and appropriate initial and iteration termination conditions. This method can almost deal with all measurement data of standard geometric element including the shapes and geometric tolerances.

5 THE MEASUREMENT OF THIN SOFT THROUGH-HOLE

At present, to deal with the measurement of all kinds of holes, researchers attempted to adopt some new approaches and some new sensors. Such as, the digital image method[6,7], the laser detection method[8],the pneumatic measurement method[9], the micro sensor method[10], and so on. Nevertheless, for those kinds of tiny thin and soft through-holes, these methods don't work effectively when both its dimension and spatial location are needed to be tested. Besides, on some practical measurement sites, the traditional plunged-bar method is still being applied. Unfortunately, it is obvious that this method has some deficiencies.

(1) The plunged-bar needs to be manufactured with the measured hole in pairs in order to guarantee gapless fit.

(2) For those tiny thin and soft holes, this method will lead to a large error even fails.

(3) This method will produce an indirect measurement error.

For this machine, while measuring the through-hole with CCD attached a bottom-light device, only when the centerline of hole is parallel to the optical axis of CCD, the image of hole is a perfect circle. Or else, the image is an ellipse. Moreover, the bigger the angle between optical axis and centerline of hole becomes, the shorter the minor axis of ellipse goes. By combining with the postures of AB axes, the optical axis of CCD can be a vector with arbitrary direction. Based on the fact, in order to evaluate the "roundness" level of a hole, an evaluating function method is proposed.

$$F(\alpha, \beta) = \min_{\substack{\alpha \in [-\alpha_0/2, +\alpha_0/2] \\ \beta \in [-\beta_0/2, +\beta_0/2]}} \left\{ \sum_{i=1}^n (|\sqrt{(x_i - x_0)^2 + (y_i - y_0)^2} - r_0|) \right\} \quad (20)$$

Where α and β denote the angle locations of AB axes respectively, α_0 and β_0 mean the angle ranges of AB axes severally, (x_i, y_i) are the edge point coordinates of tested hole,

(x_0, y_0) are centre coordinates of theoretical circle with radius r_0 .

The measurement steps:

(1) Drive A axis at given step angle. At each angle location, adjust the focal length to capture clear image of tested hole with autofocus algorithm.

(2) Calculate the value of evaluation function. So achieve a set of values of evaluation function at different angle locations.

(3) By the method of curve fitting, obtain the angle α_0 , at which the value of evaluation function is minimum.

(4) Similarly, obtain the angle β_0 .

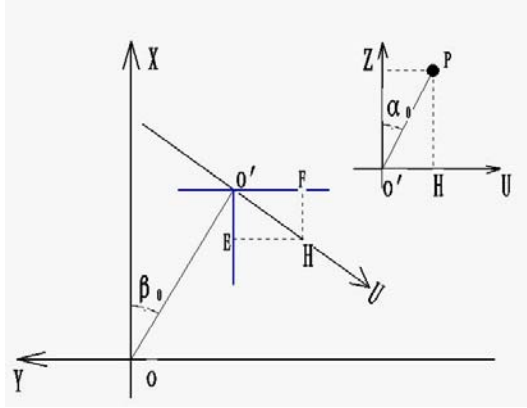


Fig. 6 The coordinate system of measuring hole

With reference to Fig.6, the point O is the rotary center of B axis, O' is the rotary center of A axis. $O'P$ denotes the orientation of optical axis of CCD. After α_0 and β_0 are known, suppose the orientation angles of center line of hole are $(\theta_x, \theta_y, \theta_z)$.

$$O'H = O'P \cdot \sin \alpha_0 \quad (21)$$

$$O'E = O'H \cdot \sin \beta_0 \quad (22)$$

$$O'F = O'H \cdot \cos \beta_0 \quad (23)$$

$$\cos \theta_x = -\frac{O'E}{O'P} \quad (24)$$

$$\cos \theta_y = -\frac{O'F}{O'P} \quad (25)$$

Substitute equation (21) and (22) into (24).

$$\cos \theta_x = -\frac{O'E}{O'P} = -\sin \alpha_0 \cdot \sin \beta_0 \quad (26)$$

Substituted equation (21) and (23) into (25).

$$\cos \theta_y = -\frac{O'F}{O'P} = -\sin \alpha_0 \cdot \cos \beta_0 \quad (27)$$

Hence, the orientation angles of center line of hole can be respectively written as.

$$\begin{cases} \theta_x = \arccos(-\sin \alpha_0 \cdot \sin \beta_0) \\ \theta_y = \arccos(-\sin \alpha_0 \cdot \cos \beta_0) \\ \theta_z = \alpha_0 \end{cases} \quad (28)$$

It can be seen that the angle between two arbitrary holes can be detected easily by this approach.

6 THE EXPERIMENTS

The designed and built five-coordinate measuring machine is present in Fig.7. The laser probe adopts CONO probe with HD25 lens coming from Israel. Its working parameters are listed in table 1. The CCD is Hitachi KP-F140 with 1392x1024 pixels.

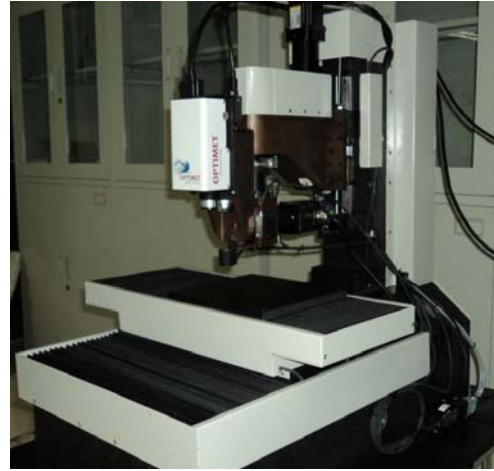


Fig.7 The five-coordinate measuring machine

Table1. The working parameters of laser probe

type	resolution	repeatability	range	standoff
Cono+HD25	0.1um	0.2um	0.6mm	14mm

The parameters of genetic algorithm are set as: population size is 500, crossover probability is 0.5, mutation probability is 0.05, penalty factor

$M = 10^4$. Under four postures of laser probe, ball center coordinates are listed in table 2.

Table 2. The ball center coordinates

$t(mm)$	$(\theta_a, \theta_b)(deg\ ree)$	$S_1(mm)$
0	(0, 0)	(0.001743,0.002189,-4.725415)
0.2	(90, 0)	(0.088509,-30.046754 ,4.432010)
0.4	(-90, 0)	(-0.012881, 9.609871, 25.132104)
0.6	(90, 90)	(-139.878714,-130.717940,4.430974)

The calibration results of system geometric parameters are presented below.

$$\Delta\theta_b = -0.722465$$

$$\Delta y_{32} = 0.782104$$

$$\begin{bmatrix} l \\ m \\ n \end{bmatrix} = \begin{bmatrix} 0.109543 \\ 0.047720 \\ 0.976634 \end{bmatrix}$$

$$(x_{43}, y_{43}, z_{43}) = (119.982704, 9.864540, 20.204917)$$

$$(x_0, y_0, z_0) = (-119.961064, -9.877542, 15.479502)$$

In order to test the repeatability of this machine, a $\phi 12$ standard steel ball with less than $0.05\ \mu m$ sphericity error is tested. The measurement path is shown in Fig.8.

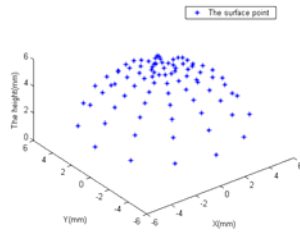


Fig.8 The measuring path

Six times results are listed in table 3.

Table 3. The measuring results of standard ball

No.	1	2	3	4	5	6
Radius(mm)	5.9998	6.0004	5.9996	6.0012	6.0007	6.0003

It can be seen that the repeatability of this machine is within $1.6\ \mu m$.

A tested object shown in Fig.9, which is glued by two cylindrical pins with 4mm diameter, is detected by this machine. The testing items include the diameter, cylindricity of each cylinder and the angle between them. Three times measuring results are shown in table 4.



Fig.9 The tested cylinders

Table 4. The three times measuring results

No.	name	Diameter (mm)	Cylindricity (mm)	Angle (degree)
1	Cylinder 1	4. 0026	0.0032	86.7653
	Cylinder 2	4. 0011	0.0023	
2	Cylinder 1	4. 0014	0.0037	86.7443
	Cylinder 2	3.9998	0.0026	
3	Cylinder 1	4. 0020	0.0027	86.7606
	Cylinder 2	4. 0007	0.0021	

The second tested object consists of two thin through-holes with 0.1 mm depth shown in Fig.10. Their materials are both brass. The testing items involve the diameter, the roundness of each hole, and the angle between their axis lines. The testing results are presented in table 5. Fig.11 illustrates the relationship between the evaluation function values and different locations of A axis. Fig.12 reveals the relationship between the evaluation function values and different locations of B axis.



Fig.10 The tested holes

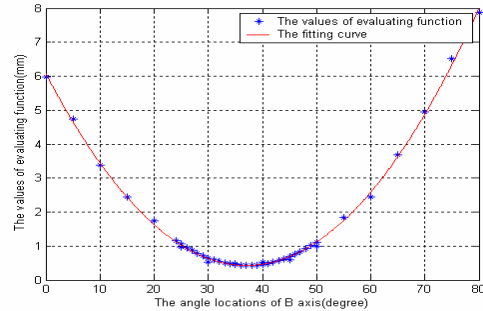


Fig.11 The values of evaluating function for A axis

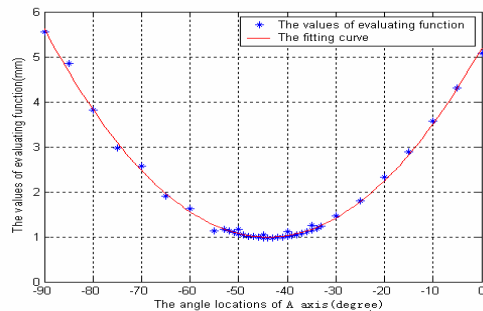


Fig.12 The values of evaluating function for B axis

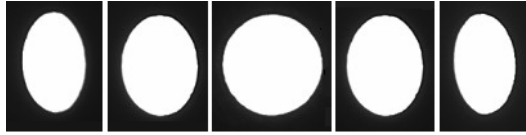


Fig.13 The images of hole at different postures

Table 5 The measuring results of two through-holes

	No.1 hole	No.2 hole
diameter(mm)	0.2505	0.2502
roundness(mm)	0.00341	0.00274
posture of CCD	$\alpha_0 = -43.7182$ $\beta_0 = 37.0763$	$\alpha_0 = 36.0462$ $\beta_0 = -26.3286$
orientation cosine	(0.4167, 0.5514, 0.7227)	(0.2610, -0.5274, 0.8085)
angle(degree)	66. 2774	

7 THE CONCLUSIONS

(1) A novel type compact five-coordinate measuring machine is designed and built in this paper. Its mechanical structure and measurement model are introduced in detail.

(2) An improved genetic algorithm is utilized to solve the unknown parameter of measurement model.

(3) The Quasi-Newton method is used to process the measured data.

(4) A new method of testing thin and soft through-holes is proposed and discussed.

(5) The final experiments illustrate the characteristics of this machine as well as the feasibility and validity of mentioned algorithms and theories.

ACKNOWLEDGEMENT

The author wishes to express gratitude to China Academy of Engineering Physics, which has supported this work.

REFERENCES

[1] Guoxiong Zhang. Development orientations of coordinate measuring techniques. *Infrared and Laser Engineering*, 2008(37): 1-5.

[2] Guoxiong ZHANG. Three-coordinate measuring machine. Tianjin University Press.

[3] Li D H, Fukushima M. A modified BFGS method and its global convergence in nonconvex minimization. *Journal of Computational and Applied Mathematics*, 2001, 129(1): 15-35.

[4] Byrd R, Nocedal J. A tool for analysis of quasi-Newton methods with application to unconstrained minimization. *SIAM Journal on Numerical Analysis*, 1989, 26(3): 727-739.

[5] Dai Y H. Convergence properties of the BFGS algorithm. *SIAM Journal on Optimization*, 2002, 13(3): 693-701.

[6] A.Cirello, S.Pasta. Displacement Measurement Through Digital Image Correlation and Digital Speckle Pattern Interferometry Techniques in Cold-Expanded Holes, *strain* 2008, 1~8

[7] Hang Cao, Xiaomei Chen, K.T.V.Grattan, Yujiu Sun. Automatic micro dimension measurement using image processing methods, *Measurement*, 2002(31) 71-76.

[8] Shuliang Ye, Jiubin Tan. High Precision Laser Deep-hole Diameter Measurement Based on Dynamic Abbe's principle, *Journal of Optoelectronics-Laser*, 2004(8) 971-974.

[9] Yonghui Zhang, Kuichun Liu. The Application of buoy pneumatic measuring instrument for detection of piston, *Internal Combustion Engine Parts*, 2000(3) 13-15.

[10] G.Y. Tian, Z.X. Zhao, R.W. Baines, P.Corcoran. A miniaturized sensor for deep hole diameter measurement, *Precision Engineering*, 1999(23) 236-242.

[11] Goh, F H, Phillips, N and Bell, R.The applicability of a laser triangulation probe to non-contact inspection. *International Journal Product Research*, Vol 24, No 6 (1986) 133 1 – 1348.

[12] Tsaourakis, N, Ristic, M and Besant, C B. Development of a profile gauging sensor. *International Journal of Advanced Manufacturing Technology*. Vol 3, No 2 (1988) 5 1-66.

[13] Jouaneh, M, Lemaster, R L and Dornfeld, D A. Measuring workpiece dimensions using a non-contact laser detector system. *International Journal of Advanced Manufacturing*. Vol 2, No 1 (1987) 59-74.

- [14] Xiaomin Bao, Yaming Wang. The Apple Image Segmentation Based on Minimal Error Probability Bayesian Decision-making Theory. Agricultural Engineering Journal, vol. 22, pp.122-124, 2006.
- [15] G. Y. Sirat and D. Psaltis, "Conoscopic holography," Optics letters 10(4), 1985.